Confinement Measurements and MHD Simulations of Oscillating-Field Current Drive in a Reversed-Field Pinch*

K. J. McCollam 1), J. K. Anderson 1), D. L. Brower 2), D. J. Den Hartog 1), W. X. Ding 2), F. Ebrahimi 1), J. A. Reusch 1), J. S. Sarff 1), H. D. Stephens 1), D. R. Stone 1)

1) Department of Physics, University of Wisconsin, Madison, USA
2) Department of Physics and Astronomy, University of California, Los Angeles, USA

Email of main author: kmccollam@wisc.edu

Abstract. Oscillating-field current drive (OFCD) is a proposed method of steady-state plasma sustainment wherein poloidal and toroidal AC loop voltages are applied to inject net magnetic helicity in order to produce a DC toroidal plasma current with magnetic relaxation. OFCD is added to reversed-field pinch (RFP) plasmas sustained by standard toroidal induction in the MST device and, with the proper phase δ between the two AC voltages, can increase the plasma current by up to about 10%. The time evolution of electromagnetic and thermal equilibrium profiles and magnetic fluctuations is measured and analyzed for different OFCD phases and for OFCD off. For $\delta \approx \pi/8$, the phase of the maximum added plasma current but not the maximum helicity-injection rate, magnetic fluctuations are somewhat reduced and energy confinement based on electron measurements is slightly improved compared to that in the standard RFP. By contrast, for $\delta = \pi/2$, which is the phase of the maximum helicity-injection rate, the helicity-decay rate is also observed to be maximum and the added plasma current is smaller, as magnetic fluctuation activity is increased and confinement is degraded. These experiments have been numerically modeled with nonlinear, 3D, resistive MHD, and the calculated dependence of the added current on the OFCD phase agrees with experiment.

1. Introduction

An efficient method of plasma current drive consistent with good energy confinement is an important goal in developing the reversed-field pinch (RFP) [1] concept. Oscillating-field current drive (OFCD) was proposed [2] in the context of RFPs as a type of steady-state plasma sustainment wherein poloidal and toroidal AC loop voltages are applied, injecting net magnetic helicity, in order to produce a DC toroidal plasma current. OFCD is potentially efficient at high plasma temperature and may provide the only feasible possibility of steady-state current drive for the RFP, which has only a small neoclassical bootstrap effect. However, the importance of magnetic relaxation to the OFCD mechanism, detailed in nonlinear resistive-MHD calculations [3], suggests that transport associated with magnetic turbulence might prevent good energy confinement, although the confinement has not yet been modeled in nonlinear MHD with finite thermal pressure. Full sustainment by OFCD is beyond present experimental capability due to the large size of the oscillations required at the operative plasma temperatures. OFCD was added to RFPs sustained by standard toroidal induction in order to increase the plasma current by about 5% in the ZT-40M device [4] and by up to about 10% [5] in the MST device [6], as shown in FIG. 1.

OFCD can be described in terms of magnetic helicity injection, where the helicity $K = \int \boldsymbol{A} \cdot \boldsymbol{B} \mathrm{d}v$ is related to the linkage of flux of the magnetic field $\boldsymbol{B} = \boldsymbol{\nabla} \times \boldsymbol{A}$ in a volume v. Since plasma current tends to increase with increased K, helicity injection is a type of current drive. The time derivative is written $K' = 2(V_\phi \Phi - \int \eta \boldsymbol{J} \cdot \boldsymbol{B} \mathrm{d}v)$ as an inductive injection rate, where V_ϕ

*This work was supported by the US DOE.

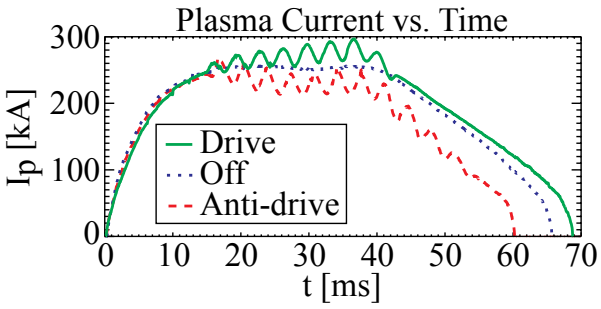

FIG. 1. Time dependences of plasma current for OFCD drive, off, and anti-drive cases in MST experimental pulses (from [5]).

is a loop voltage applied along a toroidal magnetic flux Φ, minus a decay rate due to resistivity η for the current density $\boldsymbol{J} \propto \boldsymbol{\nabla} \times \boldsymbol{B}$ along $\boldsymbol{B}$. In OFCD both the loop voltages $\widehat{V}_\phi \cos(\omega t + \delta)$ and $\widehat{V}_\theta \cos(\omega t) = -\Phi'(t)$ are oscillated, leading to an oscillating $K'(t)$ with a cycle-average $\langle K' \rangle = (\widehat{V}_\phi \widehat{V}_\theta / \omega) \sin\delta$, with maximum net injection for $\delta = \pi/2$ and maximum net ejection for $\delta = -\pi/2$. In full OFCD sustainment this injection alone balances resistive decay, and in partial sustainment it adds to the background injection from standard toroidal induction, $2\langle V_\phi \rangle \langle \Phi \rangle$.

Another, more detailed, view of OFCD focuses on its interaction with magnetic relaxation as the current drive mechanism [3]. The applied voltages set up an axisymmetric, oscillating equilibrium radial pinch flow $\boldsymbol{U}$ in tandem with an oscillating equilibrium $\boldsymbol{B}$, producing a cycle-average electromotive field (EMF) $\sim \langle \boldsymbol{U} \times \boldsymbol{B} \rangle_\parallel$ parallel to the cycle-average $\langle \boldsymbol{B} \rangle$. This drives edge current and destabilizes nonaxisymmetric magnetic fluctuations, which induce their own EMF driving net current throughout the volume, including the core. Thus, as the fluctuations redistribute injected current and tend to flatten the profile of $\lambda \propto J_\parallel / B$, magnetic relaxation is integral to the functioning of OFCD. This motivates the study of its confinement properties, which may be affected by transport along stochastic magnetic fields expected to occur with the relaxation. Also, the inherent coupling of OFCD with magnetic relaxation is a unique example of the phenomenon of interaction between control methods and plasma self-organizing responses, which is of general importance in magnetic confinement research.

This paper discusses recent experimental and theoretical results on partial OFCD sustainment of RFPs [7] in the MST device. The first main topic is a set of nonlinear, 3D, resistive-MHD simulations of previous OFCD experiments on MST. These calculations broadly reproduce the experimental observations, and in particular match the phase dependence of the added current, with the maximum current at $\delta \approx \pi/8$ rather than $\delta = \pi/2$, the phase of the maximum helicity-injection rate. The second main topic is the measurement in MST experiments of the confinement properties of OFCD for different phases compared to the standard RFP without OFCD. Energy confinement values are calculated from time-resolved equilibrium reconstructions done using internal magnetic and electron thermal measurements, and related to the observed magnetic fluctuation activity. For phases near $\delta = \pi/8$, for which magnetic activity is relatively low, the confinement is slightly improved relative to the standard case, whereas for $\delta = \pi/2$ it is degraded, apparently due to increased magnetic activity induced by the applied oscillations in that case.

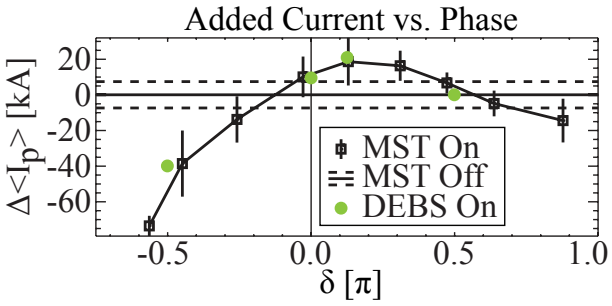

FIG. 2. Phase dependence of added plasma current in ensembled MST experiments (from [5]) and in DEBS modeling thereof (from [7]). The uncertainty estimate for the OFCD-case is shown by the dashed lines.

2. MHD Simulations and the Phase Dependence of Added Current

In OFCD experiments on MST the most added plasma current is observed at a phase of $\delta \approx \pi/8$, with the phase dependence shown in FIG. 2. This implies a complicated phase dependence of the helicity balance, in particular the helicity-decay rate, since the added current is small at $\delta = \pi/2$, the phase of the maximum helicity-injection rate. Also shown are results from nonlinear simulations of these experiments [7] using DEBS, a 3D, resistive-MHD code [8]. The agreement between the modeling and the experiment is good, although the details behind the agreement are not completely clear. The code results are also similar in most other respects to the experimental results, for instance the phase dependence of overall magnetic activity, which for the experiment is discussed below. However, one difficulty in interpreting the agreement in the phase dependence of the added current arises because the code assumes, for all cases, the same spatially profiled plasma resistivity η, which means that the phase dependence of the cycle-average helicity-decay integral $\int \langle \eta \boldsymbol{J} \cdot \boldsymbol{B} \rangle \, \mathrm{d}v$ is entirely due to the phase dependence of $\langle \boldsymbol{J} \cdot \boldsymbol{B} \rangle$. Meanwhile, calculations based on measurements from similar experiments (discussed below) imply that most of the phase dependence of $\int \langle \eta \boldsymbol{J} \cdot \boldsymbol{B} \rangle \, \mathrm{d}v$ is due to the phase dependence of η rather than that of $\boldsymbol{J} \cdot \boldsymbol{B}$. Because of the lack of a reliable effective-charge Z_{eff} measurement, the calculations for the experiment assume for all cases the same, uniform Z_{eff}, and so perhaps do not accurately reflect the actual, experimental phase dependence of $\eta \sim Z_{\mathrm{eff}} T_{\mathrm{e}}^{-3/2}$, even though the electron temperature T_{e} was measured. Another conceivable possibility would be the involvement of a more fundamental, self-organization mechanism such that the maximum acceptable rate of helicity increase is not strongly dependent on the details of the different profiles. These and other issues in comparing the MHD simulations to the experiments, as well as possible ways to improve both the future simulations and the experimental measurements, are under consideration.

3. Magnetic Fluctuations, Equilibrium Evolution, and Confinement Measurements

Magnetic fluctuation activity is modulated by the OFCD oscillations and interacts with the equilibrium evolution in a phase-dependent way. This is shown in FIG. 3, a plot of the time dependences of the toroidal V_ϕ and poloidal V_θ loop voltages, a flatness parameter α for a 1D, relaxed-state model of the $\lambda \propto J_\parallel / B$ profile, and magnetic-fluctuation amplitudes $B_{m=0}$ for the edge-resonant poloidal mode number $m = 0$, for two OFCD cases, $\delta = \pi/8$ and $\delta = \pi/2$, and the standard RFP with OFCD off. For the standard RFP there is a quasiperiodic sawtooth relaxation cycle [9], evident as the spikes in the plot, responsible for maintaining a relatively

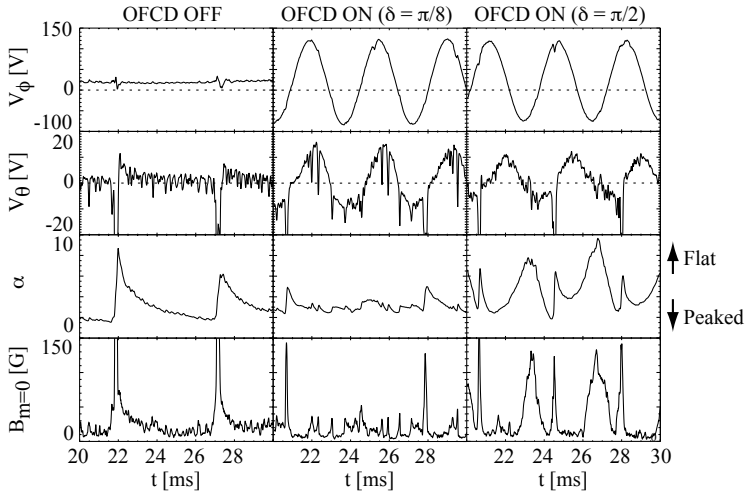

FIG. 3. Time dependences of (from top to bottom) toroidal V_ϕ and poloidal V_θ loop voltages, a flatness parameter α for the $\lambda \propto J_\parallel/B$ profile, and magnetic-fluctuation amplitudes $B_{m=0}$ for the edge-resonant poloidal mode number $m = 0$, for the standard RFP with OFCD off (left column) and the OFCD cases of $\delta = \pi/8$ (middle column) and $\delta = \pi/2$ (right column) in MST experimental pulses.

flat time-average λ profile despite the fact that the applied toroidal induction continually leads it toward being more peaked. Each sawtooth reconnection event is a sharp increase in magnetic fluctuations and flattening of the λ profile with transiently increased magnetic stochasticity and decreased energy confinement. In the OFCD cases the sawtooth cycle becomes strongly periodic, entrained to the applied AC loop voltages, and overall magnetic activity is modulated depending on δ. For $\delta = \pi/2$, in addition to the entrained sawteeth, large, relatively long surges in $m = 0$ amplitudes occur between sawteeth, along with similar increases in core-resonant $m = 1$ mode amplitudes (not shown in FIG. 3). These fluctuations are apparently driven directly by the applied voltages, which strongly modulate the λ profile. For $\delta = \pi/8$, the sawteeth are entrained but somewhat suppressed, the time-average $m = 0$ amplitudes are decreased relative to the OFCD-off case, and the λ profile is more quiescent. As shown below, this evidently leads to slightly improved confinement for phases near $\delta = \pi/8$. These results are reminiscent of the theoretical idea of using OFCD to suppress magnetic activity [10].

Within a cycle of OFCD at $\delta = \pi/4$, which is near the observed maximum in added plasma current, the measured electron pressure $\sim n_e T_e$ profile oscillates with the applied voltages by about 50% of the cycle average, which average is slightly larger than the time average for OFCD

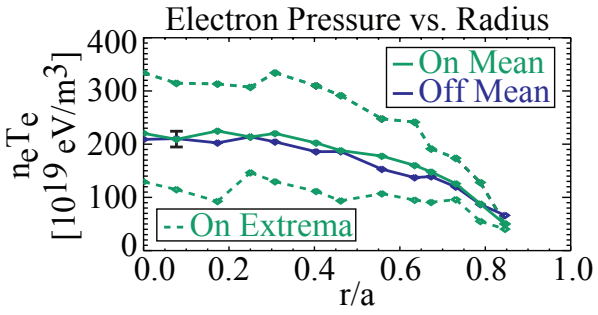

FIG. 4. Cycle-average and cycle-extreme radial profiles of oscillating electron pressure $\sim n_e T_e$ for OFCD at $\delta = \pi/4$ compared to the time-average for OFCD off in ensembled MST experiments.

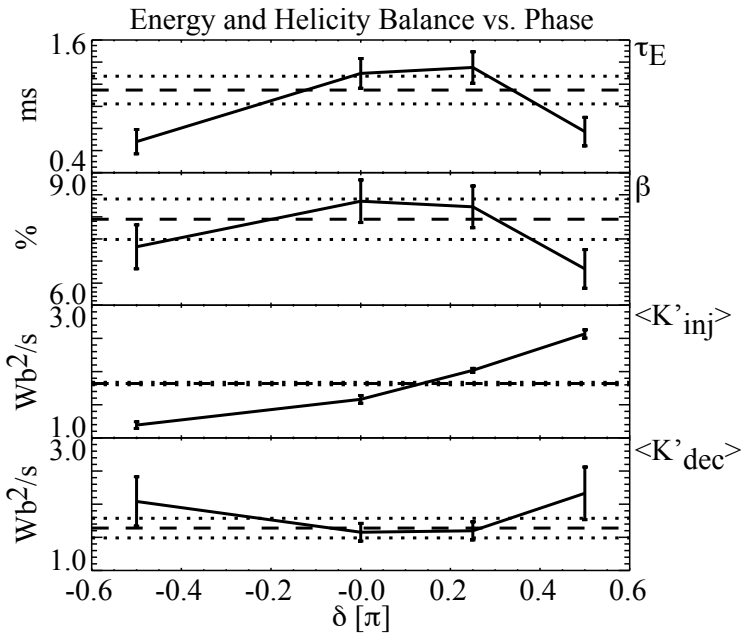

FIG. 5. Phase dependences of (from top to bottom) cycle-averaged energy confinement time τ_E, normalized thermal pressure β, helicity-injection rate $\langle K'_{inj}\rangle$, and helicity-decay rate $\langle K'_{dec}\rangle$ in ensembled MST experiments (from [7]). Values for the OFCD-off case are shown as dashed lines and their uncertainty estimates as dotted lines.

off, as shown in FIG. 4. This time-resolved profile information is measured with multichord far-infrared (FIR) interferometry [11] for the electron density n_e and multichord Thomson-scattering spectroscopy [12] for the electron temperature T_e. In OFCD both quantities tend to oscillate in phase with each other, and the T_e oscillation tends to be larger than the n_e oscillation, each normalized to its cycle average. Detailed analysis implies the thermal pressure oscillation is mainly the result of cyclic compressional heating by OFCD rather than modulated Ohmic heating [7]. For the case of $\delta = \pi/2$ (not shown in FIG. 4), the pressure is suppressed overall relative to the OFCD-off case, which is associated with the high magnetic activity induced by the oscillations in that case.

For OFCD phases near $\delta = \pi/8$, the phase of the maximum added plasma current, the measured cycle-average energy confinement time τ_E and normalized thermal pressure β are slightly increased relative to those in the standard RFP without OFCD, as shown in FIG. 5, a plot of the phase dependences. These quantities, calculated from cycle-averages of time-resolved equilibrium reconstructions [13] that used internal magnetic measurements [14, 15] and electron thermal measurements, are defined $\tau_\mathrm{E} \equiv \langle W_\mathrm{th}\rangle / \langle P_\mathrm{th} - W'_\mathrm{th}\rangle$, where the thermal energy content W_th is taken to be twice the measured electron energy and P_th is the heating rate of the electrons, and $\beta \equiv 2\mu_0\langle\bar{p}\rangle/\langle B^2(a)\rangle$, where $\bar{p}$ is twice the spatially averaged electron thermal pressure and $B(a)$ is the magnetic field at the wall. The slight improvements in confinement properties are consistent with the relatively small levels of magnetic activity for the OFCD phases near $\delta = \pi/8$ discussed above. For the case $\delta = \pi/2$, the decreased confinement is evidently due to the large increases in magnetic activity induced by OFCD in that case, also discussed above.

Also shown in FIG. 5 are phase dependences of the cycle-average helicity-injection rate $\langle K'_\mathrm{inj}\rangle = 2\langle V_\phi \Phi\rangle$ and helicity-decay rate $\langle K'_\mathrm{dec}\rangle = 2\int\langle \eta \boldsymbol{J}\cdot\boldsymbol{B}\rangle \mathrm{d}v$. Note that $\langle K'_\mathrm{inj}\rangle$ is not purely sinu-

soidal in part because the sinusoidal OFCD part $(\widehat{V}_\phi \widehat{V}_\theta/\omega)\sin\delta$ is added to the background part $2\langle V_\phi\rangle\langle\Phi\rangle$, which itself is observed to have a nontrivial OFCD phase dependence. It is seen that the case of $\delta = \pi/2$ has not only the maximum $\langle K'_{\text{inj}}\rangle$ as expected, but also the maximum $\langle K'_{\text{dec}}\rangle$, which is mostly due to an increased resistivity η, brought about the by higher magnetic activity and lower confinement in that case. Conversely, phases near $\delta = \pi/8$ have small values of both $\langle K'_{\text{dec}}\rangle$ and $\langle K'_{\text{inj}}\rangle$. It seems that a portion of the added plasma current in these cases might be caused not by the OFCD helicity injection itself but by a drop in plasma resistance to the background toroidal induction, brought about by the slightly higher time-average temperatures consistent with the slightly improved confinement. For these phases the cycle-average background toroidal loop voltage $\langle V_\phi\rangle$ is observed to drop by several percent while the toroidal flux $\langle\Phi\rangle$ goes up by about the same fraction. The issue is difficult to clarify in part because the signals are small.

4. Future Work and Summary

Initial experiments are underway in which OFCD is applied using a new programmable power supply for V_θ on MST to enable improved waveform control, nonsinusoidal oscillations, and higher OFCD input power. With improved waveform control, different OFCD conditions can be tested more easily than with the previous hardware, which should expand the meaningful experimental parameter space. Using nonsinusoidal oscillations may allow progress in understanding and controlling OFCD's effect on magnetic fluctuation activity. Aside from its inherent importance for magnetic relaxation and self-organization generally, the phenonmenon of induced magnetic activity seems at present to place a key limit on the effectiveness of OFCD for the maximum helicity-injection rate at $\delta = \pi/2$. Therefore more facility in this regard might provide a way to improve OFCD's performance further. Higher OFCD input power should provide not only the possibility of increased performance but also larger OFCD signals generally, which could help in understanding how the current-drive mechanism works in the experiment. In the longer term, further power-supply improvements could provide longer MST pulse lengths with full programmability, which would be expected, for the same OFCD conditions, to enable more added current and better characterization of the current drive.

Modeling OFCD numerically has been important in elucidating the underlying current-drive mechanism and in particular the role of magnetic relaxation. Future simulations of new OFCD scenarios in MST, for instance those with nonsinusoidal waveforms or higher input power, could help make experimental plans more efficient. The MHD simulations discussed above showed good agreement with key aspects of the experiments, although it may be useful to include thermal effects in future runs to better understand the role of energy transport in determining the outcomes with different OFCD conditions. In the longer term, given the incapability of providing OFCD amplitudes large enough for full sustainment in present experiments, finite-pressure MHD simulations of full sustainment would be useful in informing expectations about OFCD confinement properties at higher plasma temperatures. Continuing the simulation effort along these lines is under consideration.

Summarizing, OFCD is prospectively an efficient, steady-state sustainment method for the RFP that uses applied poloidal and toroidal AC loop voltages to inject net magnetic helicity in order to drive a DC plasma current. Because it relies on magnetic relaxation to function, the question of its confinement properties for full sustainment at high plasma temperature is an important one yet to be answered. In MST experiments where OFCD is added to RFPs sustained by toroidal

induction at phases of $\delta \approx \pi/8$, it is found to increase the plasma current by up to about 10% while decreasing $m = 0$ magnetic fluctuations and slightly improving the energy confinement calculated from electron measurements. At $\delta = \pi/2$, the phase of the maximum helicity-injection rate, relatively large magnetic fluctuations are induced and the energy confinement is degraded. Nonlinear, 3D, resistive-MHD simulations of the MST experiments show good agreement with the experimental results, in particular the phase dependence of the added plasma current.

References

[1] BODIN, H.A.B., NEWTON, A.A., "Reversed-field-pinch research", Nucl. Fusion **20** (1980) 1255.

[2] BEVIR, M.K., GRAY, J.W., "Relaxation, Flux Consumption and Quasi Steady State Pinches" (Proc. RFP Theory Workshop, Los Alamos, 1980), LA-8944-C, LANL, Los Alamos (1982) 176.

[3] EBRAHIMI, F., et al., "The three-dimensional magnetohydrodynamics of ac helicity injection in the reversed field pinch", Phys. Plasmas **10** (2003) 999.

[4] SCHOENBERG, K.F., et al., "Oscillating field current drive experiments in a reversed field pinch", Phys. Fluids **31** (1988) 2285.

[5] MCCOLLAM, K.J., et al., "Oscillating-Field Current-Drive Experiments in a Reversed Field Pinch", Phys. Rev. Lett. **96** (2006) 035003.

[6] DEXTER, R.N., et al., "The Madison Symmetric Torus", Fusion Technol. **19** (1991) 131.

[7] MCCOLLAM, K.J., et al., "Equilibrium evolution in oscillating-field current-drive experiments", Phys. Plasmas **17** (2010) 082506.

[8] SCHNACK, D.D., et al., "Semi-implicit Magnetohydrodynamic Calculations", J. Comput. Phys. **70** (1987) 330.

[9] HO, Y.L., CRADDOCK, G.G., "Nonlinear dynamics of field maintenance and quasiperiodic relaxation in reversed-field pinches", Phys. Fluids B **3** (1991) 721.

[10] EBRAHIMI, F., PRAGER, S.C., "Current profile control by alternating current magnetic helicity injection", Phys. Plasmas **11** (2004) 2014.

[11] JIANG, Y., et al., "Interferometric measurement of high-frequency density fluctuations in Madison symmetric torus", Rev. Sci. Instrum. **70** (1999) 703.

[12] REUSCH, J.A., et al., "Multipoint Thomson scattering diagnostic for the Madison Symmetric Torus reversed-field pinch", Rev. Sci. Instrum. **79** (2008) 10E733.

[13] ANDERSON, J.K., et al., "Equilibrium reconstruction in the Madison Symmetric Torus reversed field pinch", Nucl. Fusion **44** (2004) 162.

[14] DEN HARTOG, D.J., et al., "Advances in neutral-beam-based diagnostics on the Madison Symmetric Torus reversed-field pinch (invited)", Rev. Sci. Instrum. **77** (2006) 10F122.

[15] DENG, B.H., et al., "High-speed three-wave polarimeter-interferometer diagnostic for Madison symmetric torus", Rev. Sci. Instrum. **77** (2006) 10F108.